AAC Accepts, published online ahead of print on 23 June 2014
Antimicrob. Agents Chemother. doi:10.1128/AAC.03233-14

1,4-azaindole: potential drug candidate for the treatment of tuberculosis

Monalisa Chatterji,[1*#] Radha Shandil,[2*#] M. R. Manjunatha,[3] Suresh Solapure,[2] Vasanthi Ramachandran,[1] Naveen Kumar,[2] Ramanatha Saralaya,[2] Vijender Panduga,[2] Jitendar Reddy,[2] Prabhakar KR,[2] Sreevalli Sharma,[1] Claire Sadler,[4] Christopher B. Cooper,[5] Khisi Mdluli,[5] Pravin S. Iyer,[3] Shridhar Narayanan,[1] and Pravin S. Shirude[3*#]

[1]Department of Biosciences, IMED Infection, AstraZeneca India, Bellary Road, Hebbal, Bangalore-560024, India
[2]DMPK and Animal Sciences, IMED Infection, AstraZeneca, India
[3]Department of Medicinal Chemistry, IMED Infection, AstraZeneca, India
[4]Safety Assessment, IMED, AstraZeneca, Alderly Park, Mereside, UK
[5]Global Alliance for TB Drug Development, New York, NY, USA

[#] Equal contribution
*Corresponding authors
monalisa.chatterji@astrazeneca.com, radha.shandil@astrazeneca.com and pravin.shirude@astrazeneca.com
Tel: +91 80 66213000
Fax: +91 80 23621214

Abstract

New therapeutic strategies against multidrug-resistant (MDR) and extensively drug-resistant (XDR) *Mycobacterium tuberculosis* (Mtb) are urgently required to combat the global tuberculosis (TB) threat. Towards this end, we have previously reported identification of 1,4-azaindoles, a promising class of compounds with potent anti-tubercular activity through non-covalent inhibition of decaprenylphosphoryl-β-D-ribose2'-epimerase (DprE1). Further, the series was optimized to improve physico-chemical properties and pharmacokinetics in mice. Here, we describe shortlisting of a potential clinical candidate, compound **2**, that has potent cellular activity, drug-like properties, efficacy in a chronic mouse and rat TB infection models with minimal *in vitro* safety risks. We also demonstrate that the compounds including compound **2**, has no antagonistic activity with other anti-TB drugs. Moreover, compound **2** shows synergy with PA-824 and TMC207 *in vitro* and the synergy effect was translated *in vivo* with TMC207. In addition, the series is predicted to have low clearance in human and the predicted human dose for the compound **2** is ≤1gm/day. Together, our data suggests that 1,4-azaindole (compound **2**) is a promising candidate for development of a novel anti-TB drug.

INTRODUCTION

38 Studies have revealed *Mycobacterium tuberculosis* (Mtb), an opportunistic intracellular
39 bacterium, has originated thousands of years ago; genetic analysis of more than 250
40 contemporary strains, indicate its origin with the emergence of Homo sapiens in Africa more
41 than 70,000 years ago.[1] The spread, evolution and existence of the bacterium to this day, is
42 an evolutionary success, as well as, a serious threat to humanity.[1] Even today, tuberculosis
43 (TB) is a leading cause of mortality in the world, second only to HIV.[1] WHO reported 1.3
44 million deaths in 2012.[2] TB has emerged as a global health emergency as Mtb has acquired
45 resistance to every drug that has been introduced against it.[3] Moreover, multi- (MDR) and
46 extreme- (XDR) drug resistant strains have made TB therapy ineffective, moving the disease
47 back to the pre-antibiotic era. The long duration of therapy and associated toxicities, has
48 challenged patients' compliance and further assisted development of resistance. A
49 simplified, relatively safe and shorter duration of therapy is required to combat TB threat.[4]
50 Drugs that work by novel mechanisms hence, active on drug resistant strains are urgently
51 needed to treat patients with drug resistant TB.

52 Mtb has a characteristic and complex cell wall architecture involved in multiple functions
53 related to cellular physiology and pathogenesis.[5] Isoniazid, a critical drug in the first line
54 therapy, inhibits biosynthesis of mycolic acid, a critical component of cell wall.[6,7] Ethambutol,
55 another drug in the first line therapy, also inhibits cell wall synthesis.[6,7] Enzymes that are
56 involved in cell wall biogenesis and/or function have emerged as potential targets for
57 discovery of antimycobacterials, one such target is decaprenylphosphoryl-β-D-ribose2'-
58 epimerase (DprE1).[6,7] DprE1 along with DprE2 catalyzes the epimerization of
59 decaprenylphosphoryl-D-ribose to decaprenylphosphoryl-D-arabinose, the sole arabinose
60 donor for cell wall synthesis.[8] A number of DprE1 inhibitors have been reported in the
61 literature that are bactericidal *in vitro* and in mouse TB infection models, building confidence
62 for this target.[9-12] Benzothiazinones (e.g. BTZ043), covalent inhibitors of the DprE1 enzyme,
63 were instrumental in the discovery of the target.[9] The nitro-group of this scaffold is converted
64 to nitroso subsequently forming a covalent link with cysteine at 387 position of the enzyme.[9]
65 PBTZ, an improved analogue of BTZ043 has been shown to be effective in an animal model
66 for TB with a synergistic effect in combination with TMC207.[12] PBTZ is in the pre-clinical
67 phase of development under the sponsorship of iM4TB (Innovative Medicines for
68 Tuberculosis). TCA1, a non-covalent inhibitor of DprE1 also inhibits MoeW - enzymes
69 involved in cell wall and molybdenum cofactor biosynthesis.[10] TCA1 is currently in a lead
70 optimization phase as part of TB alliance portfolio.[13]

71 We have previously reported a novel class of DprE1 inhibitors, 1,4-azaindoles.[11] This series
72 emerged from a scaffold morphing effort and demonstrated potent antimycobacterial activity

73 and were non-covalent inhibitors of DprE1. In addition, the target site mutations conferring
74 resistance against azaindoles and BTZ043 were distinct from each other. While C387S/G is
75 the primary residue involved in BTZ043 resistance, Y314H imparts resistance to azaindoles.
76 Cross-resistance was not observed between azaindoles and BTZ043, and azaindoles were
77 found to be equally active on drug sensitive and isoniazid/rifampicin resistant strains. A
78 robust understanding of the structure activity relationship (SAR) was used to optimize the
79 series.

80 1,4-azaindoles possess small molecular weight, low logD, excellent permeability, no CYP
81 inhibition, good oral exposures, low *in vivo* clearance (CL) in rats & dogs and low predicted
82 human CL, and no major safety liabilities as assessed by a spectrum of *in vitro* assays.
83 Moreover, the synthesis of compounds is not complex hence, expected to have low cost of
84 goods. Hence 1,4-azaindoles is an attractive class for further development towards TB
85 treatment. During lead optimization, low solubility, high mouse specific clearance and weak
86 phosphodiesterase6 (PDE6) inhibition were mitigated based on SAR understanding of 1,4-
87 azaindoles. This has led to the identification of a potential drug candidate for TB treatment.
88 In this report, the *in vivo* efficacy of the candidate drug in a chronic mouse and rat model of
89 tuberculosis has been demonstrated along with its synergy with TMC207. The minimal
90 safety risk as per the *in vitro* secondary pharmacology data, no adverse observations during
91 efficacy study, drug like properties and acceptable predicted human dose, makes 1,4-
92 azaindole a promising candidate for development.
93
94 **Materials and methods:**
95 **Synthesis of selected compounds**
96 **N-(2-hydroxyethyl)-1-((6-methoxy-5-methylpyrimidin-4-yl)methyl)-6-methyl-1H-**
97 **pyrrolo[3,2-b]pyridine-3-carboxamide (1):**
98 1-((6-methoxy-5-methylpyrimidin-4-yl)methyl)-6-methyl-1H-pyrrolo[3,2-b]pyridine-3-
99 carboxylic acid (75 mg, 0.24 mmol) was added to dichloromethane (10 mL) to give a
100 suspension. Triethyl amine (66.9 mL, 0.48 mmol) was added, followed by 1-
101 propanephosphonic acid cyclic anhydride (286 mL, 0.48 mmol). The reaction mixture was
102 stirred at RT for 5 minutes. Ethanol amine (29.0 mL, 0.48 mmol) was added and the mixture
103 was stirred at RT overnight. After completion of the reaction, the mixture was diluted with
104 DCM, washed with water and brine. The DCM layer was dried over sodium sulphate and
105 evaporated to give the crude product. The crude product was was purified by silica gel
106 column chromatography using MeOH in DCM to afford N-(2-hydroxyethyl)-1-((6-methoxy-5-
107 methylpyrimidin-4-yl)methyl)-6-methyl-1H-pyrrolo[3,2-b]pyridine-3-carboxamide as a white
108 solid (**1**) (Yield 53%).

109 ES+ MS m/z: 356.4 (M+1)

110 ^{1}H NMR (300 MHz, DMSO-d_6) δ ppm: 2.23 (s, 3 H) 2.39 (s, 3 H) 3.39 - 3.65 (m, 4 H) 3.93 (s,
111 3 H) 4.84 (t, *J*=5.09 Hz, 1 H) 5.63 (s, 2 H) 7.74 (s, 1 H) 8.12 (s, 1 H) 8.33 (s, 1 H) 8.41 (s, 1
112 H) 8.80 (t, *J*=5.65 Hz, 1 H).

113

114 **1-((6-(dimethylamino)-5-methylpyrimidin-4-yl)methyl)-N-(2-hydroxyethyl)-6-methyl-1H-**
115 **pyrrolo[3,2-b]pyridine-3-carboxamide (2):**

116 To a stirred solution of 1-((6-(dimethylamino)-5-methylpyrimidin-4-yl)methyl)-6-methyl-1H-
117 pyrrolo[3,2-b]pyridine-3-carboxylic acid (7g, 21.51 mmol) in DMF (70 mL), Ethanol amine
118 (1.97 g, 32.265 mmol), triethylamine (8.99 mL, 64.53 mmoles) and HATU (9.81 g, 25.81
119 mmoles) were added and the mixture was stirred at room temperature for 2 h. Then the
120 reaction mixture was poured into water (100 mL) and extracted with ethyl acetate (2 X
121 200mL). The organic layer was washed with brine and concentrated under reduced
122 pressure. The crude product was purified by silica gel column chromatography using MeOH
123 in DCM to afford 1-((6-(dimethylamino)-5-methylpyrimidin-4-yl) methyl)-N-(2-hydroxyethyl)-6-
124 methyl-1H-pyrrolo [3, 2-b] pyridine-3-carboxamide as a white solid (**2**) (Yield 60%).

125 ES+ MS m/z: 369.4 (M+1)

126 ^{1}H NMR (400MHz ,DMSO-d_6) δ ppm: 2.27 (s, 3 H), 2.39 (s, 3 H), 2.95 (s, 6 H), 3.45 (q, *J*=
127 5.7 Hz, 2 H), 3.54 (q, *J*= 5.2 Hz, 2 H), 4.81 (t, *J*= 5.0 Hz, 1 H), 5.52 (s, 2 H), 7.73 (s, 1 H),
128 8.09 (s, 1 H), 8.22 (s, 1 H), 8.32 (d, *J*= 1.3 Hz, 1 H), 8.79 (t, *J*= 5.6 Hz, 1 H).

129

130 **Microbiology and biochemical assays**

131 Assays to determine cellular activity (MIC, MBC), potency in intracellular THP1 model, and
132 IC_{50} fo DprE1 assay was carried out a described before.[11] IC_{50} is compound concentration
133 that results in 50% inhibition of maximum enzyme activity. MIC referes to the minimal
134 compound concentratiosn that is able to reduce cell growth by 80% or more compared to the
135 untreated cells in 7 days, MBC refers to minimal compound concentartion that shows ≥2 log
136 reduction in colony forming units in 7 days compared to cells at the start of the treatment and
137 DprE1. For MIC determination 14 drug sensitive clinical isolates, 8 isoniazid (INH^R) and one
138 rifampicin resistant (RIF^R) strains were used.

139

140 ***In vitro* combination**

141 Activity of 1,4-azaindole in combination with known anti-TB drugs was determined by
142 checkerboard titration method.[14] Briefly, in a 96-well microtiter plate, one drug was diluted
143 row wise and the second drug was diluted to obtain various combinations of two drugs in a
144 final volume of 100 µL. Each well of the micro-titre plate was inoculated with 100 µL of Mtb

145 H37Rv culture at 5 x 10^5 CFU/ml. The plates were incubated for 7 days at 37 ^{0}C. To
146 evaluate whether the paired combinations of agents had additive, synergistic, antagonistic or
147 indifferent effect in inhibiting Mtb, the fractional inhibitory concentration index (ΣFIC) using
148 the following formula was calculated.
149 $\Sigma FIC = F_A + F_B$
150 F_A = MIC of drug A in combination/MIC of drug A alone
151 F_B = MIC of drug B in combination / MIC of drug B alone
152 The synergy was defined as ΣFIC of $\leq$0.5, antagonism as a ΣFIC of $\geq$4.0, and
153 additivity/indifference (no interaction) as ΣFIC values between 0.5 and 4.0.
154 In a combination of two drugs – Indifference equals to the effect of the most active
155 component, additive equals to the sum of the effects of the individual components, synergy
156 equals to the effect of the combination that exceeds the additive effects of the individual
157 components and antagonism equals to the reduced effect of the combination in comparison
158 with the effect of the more potent individual substance.
159 All combinations showing a ΣFIC value of <1 were further plated to estimate CFUs. The $\log_{10}$
160 CFU reduction in 7 days was calculated with respect to untreated control.
161
162 ***In vitro* DMPK and safety assays**
163 *In vitro* DMPK assays to measure aqueous solubility, LogD, plasma protein binding,
164 metabolic stability (mouse/human microsomal CL_{int}; rat, dog, human hepatocyte CL_{int}), as
165 well as, safety assays to measure inhibition of hERG channel, Cytochrome P450 enzymes
166 (CYPs), and a panel of ~65 mammalian targets have been described earlier.[11]
167
168 **Pharmacokinetics (PK) and efficacy in animal models (rats and mice)**
169 Methods used for determining the pharmacokinetics in mice and rats after intraveneous
170 (IVPK) and or oral administration (POPK) of drug, as well as, *in vivo* efficacy in a mouse and
171 rat aerosol infection models of TB have been described earlier.[11,15] In both the models,
172 treatment was initiated after four weeks of infection and the total duration of treatment was
173 for 4 weeks (6 days/week). Animals were sacrificed and viable bacterial counts in the lungs
174 were enumerated.
175
176 **Pharmacokinetics (PK) in dog**
177 PK was analysed in healthy Beagle dogs, one male and one female dog per dose group.
178 For intravenous PK (IVPK), a dose of 5 µmol/kg of the test compound (**1**) was administered
179 as solution containing 5% ethanol, 30% PEG-200 & 65% phosphate buffered saline (PBS)
180 by infusion. For oral PK (POPK), 5 µmol/kg of the compound (**1**) was administered in a
181 suspension containing 0.5% hydroxypropyl methycellulose (HPMC) and 0.1% Tween in

182 water. Blood samples were collected at 5, 10, 20, 40 mins, 1, 2, 4, 6, 12 h for IVPK and 10,
183 20, 40 mins, 1, 2, 3, 4, 6, 12 h for POPK. Blood samples were centrifuged to collect plasma
184 and samples were stored at -20^{0}C until analysis using LC-MS/MS.
185
186 **Prediction of *in vivo* CL from *in vitro* CL_{int}**
187 Assuming major route of elimination to be through hepatic metabolism, blood CL in
188 preclinical species, rat and dog was predicted from *in vitro* CL_{int} (by *in vitro-in vivo* correlation
189 or IVIVC). *In vitro* CL_{int} was estimated by incubating the test compound with rat or dog
190 hepatocytes. *In vitro* CL_{int} was scaled to *in vivo* CL_{int} as follows.
191 CL_{int} *in vivo* = CL_{int} *in vitro* * scaling factors * fu_{blood}/fu_{inc}
192 The liver weight used for scaling was 40, 32 & 24 g/kg body weight in rat, dog and human
193 respectively. Hepatocellularity used for scaling was 163, 169 & 120 (X 10^6) cells/g liver in
194 rat, dog and human respectively. The fu_{blood} or free fraction in blood and fu_{plasma} (unbound
195 fraction in plasma) were assumed to be similar, while the unbound fraction in the hepatocyte
196 mix, fu_{inc} was predicted using physicochemical properties.[16] Slope and intercept from the
197 linear regression analysis of IVIVC for a large number of AstraZeneca compounds were
198 applied for final correction in the scaled *in vivo* CL_{int}. For prediction of CL, a well stirred
199 model was used, equation as described below.
200
201 $$\text{Predicted CL} = \frac{Q_h \times predicted\ \text{CLint}_{\text{in vivo}}}{Q_h + predicted\ \text{CLint}_{\text{in vivo}}}$$
202 Where, Q_h is the liver blood flow. The values of Q_h in rat, dog and human are 72, 55 & 20
203 mL/min/kg in rat, dog and human, respectively.[16]
204
205 **Human dose prediction by allometry**
206 Allometry exponent (b) and coefficient (a) were estimated by linear regression analysis of log
207 (CL) vs. log (body weight or BW) plot.
208 Equation for simple allometry: $\boxed{CL = a \times BW^b}$
209 The steady-state daily AUC required for 1.0 $\log_{10}$CFU reduction in the chronic rat TB
210 infection model, oral bioavailability (F = ratio of dose normalized AUCs after oral and IV
211 administration) in rat and human CL predicted by IVIVC were used for human dose
212 prediction as shown below.
213 Predicted human dose = (Efficacious AUC in rat*Predicted Hu CL)/F
214
215 **Results and discussion**
216 **Selection of potential drug candidate and properties**
217 The 1,4-azaindole series was identified by scaffold morphing approach as described
218 previously.[15] The potency of these compounds against Mtb was mainly improved through

219 MIC-based SAR with three points of diversification (amide side chain, a hydrophobic group,
220 and core ring substitutions). The secondary amide, referred to as the amide side chain is
221 essential for potency. It could be involved in hydrogen bonding interaction with the target
222 enzyme, DprE1. Small hydrophobic or hydrophilic amides like methyl cyclopropyl, fluoro-
223 ethyl or hydroxy ethyl amides were preferred for MIC. The hydrophobic group tolerated
224 various substituted benzyl and heteroaryl-methyl groups; however, monosubstituted benzyl
225 groups were less favoured than disubstituted benzyl groups. Substitution of a methyl or
226 methoxy group at the C-6 position of the 1,4-azaindole improved cellular potency.
227 Although 1,4-azaindoles showed excellent *in vitro* and *in vivo* efficacy against Mtb, these
228 compounds had poor aqeous solubility, showed high CL in mouse and weakly inhibited the
229 host PDE6 enzyme activity which could potentially lead to visual acuity. Therefore, the major
230 focus during lead optimization was to improve these properties while retaining Mtb potency.
231 The hydroxyethyl amide side chain was crucial to improve aqueous solubility and modulate
232 physicochemical properties of 1,4-azaindoles. In addition, the hydroxyethyl amide side chain
233 showed a significant improvement in mouse liver microsome (MLM) stability relative to
234 hydrophobic amide side chains. The improved MLM stability was attributed to the
235 compounds with lower lipophillicity as indicated by measured logDs of 2 or less. Structurally
236 diverse compounds from 1,4-azaindole series were profiled for *in vitro* PDE6 screening to
237 understand the PDE6 SAR. The result revealed that 6-methoxy-5-methylpyrimidine-4-yl
238 group at hydrophobic pocket was the primary cause of PDE6 activity. It was demonstrated
239 that replacement of 6-methoxy-5-methylpyrimidine-4-yl substituent with 6-(dimethylamino)-5-
240 methylpyrimidine-4-yl and 6-(difluoromethoxy)-5-methylpyrimidine-4-yl groups helped to
241 mitigate PDE6 activity.
242 Thus, overall from an initial hit, 1,4-azaindole series was optimized to have molecules with
243 small molecular weight, low logD, nanomolar DprE1 IC_{50}s, sub-micromolar MICs, excellent
244 permeability, no CYP inhibition, good oral exposures, low clearance in mice, rats, dogs &
245 humans and no major safety liabilities. Relatively straighforward synthesis of 1,4-azaindoles
246 with no chiral centers ensures low cost of goods, an essential attribute for an anti-TB drug.
247 Synthesis and characterization of ~250 compounds during lead optimization has led to the
248 identification of compound **2**, as a potential drug candidate for TB (Figure 1).
249
250 The specific properties of compound **2** along with an early tool compound **1** are shown in
251 Table 1. Both the compounds have logD < 2, aqueous solubility >100 μM, similar fu_{plasma},
252 nanomolar IC_{50}s against Mtb DprE1 enzyme and potent MICs and MBCs against Mtb. These
253 compounds were equally active against drug sensitive and drug resistant clinical isolates of
254 Mtb. They were also active against intracellular Mtb and showed ~1.5 Log_{10}CFU reduction
255 inside the infected THP1 cells (Table 1, Supplemental Figure 1). On the basis of *in vitro*

256 intrinsic clearance (CL_{int}) using hepatocytes from rat and dog, the predicted *in vivo* clearance
257 (CL) for compounds **1** & **2** ranged between 11 and 30% of liver blood flow (% LBF),
258 indicating low clearance (Table 2). Thus, low CL_{int} in hepatocytes correlated with observed
259 low CL (< 35% LBF) in rat and dog. Good correlation between the predicted *in vivo* CL and
260 observed *in vivo* CL supported our assumption that hepatic clearance could be the primary
261 route of elimination of these compounds. IVIVC predicted low CL in human for both the
262 compounds. High permeability in the Caco2 assay as well as > 85% oral bioavailability in
263 rat/dog predicts excellent bioavailability in human. Moreover, TB being a chronic
264 combination therapy, understanding of safety profile is critical. Cytotoxicity assay in THP-1
265 (human monocytic cell line) cells showed no inhibition at up to 100 μM. Compounds **1** & **2**
266 did not inhibit the hERG channel at up to 33 μM concentrations, suggesting a low risk of
267 cardiovascular toxicity. Compounds in this series, including **1** & **2,** did not inhibit any of the
268 cytochrome P450 (CYP450) isoenzymes. A panel of mammalian targets associated with
269 serious safety liabilities were used to test for inhibition by 1,4-azaindoles. None of the targets
270 were significantly inhibited except weak inhibition of phosphodiesterase6 (PDE6) enzyme by
271 compound **1** (PDE6 IC_{50} 4μM). As described above, mitigation of PDE6 inhibition (PDE6 IC_{50}
272 >100 μM) through systematic medicinal chemistry exploration resulted in the identification of
273 compound **2**.
274
275 ***In vitro* combination study with known TB drugs and clinical candidates**
276 Compounds **1** and **2** were tested in combination with various first & second line anti-TB
277 drugs and clinical/pre-clinical TB candidates *in vitro* namely, isoniazid, rifampicin,
278 ethambutol, streptomycin, moxifloxacin, imipenem, meropenem, BTZ043, bedaquiline
279 (TMC207), and PA824. Antagonism was not observed for any combination tested in this
280 study. For *M. tuberculosis*, translation of ΣFIC to bactericidality (reduction in CFU) was used
281 to rank order combinations. FIC values were used as a criterion to select combinations for
282 CFU plating. All combinations with ΣFIC <1 were plated for estimation of reduction in CFU
283 compared to individual drugs treated at MIC. Maximum synergy for compound 2 based on
284 CFU estimate, was observed with PA824 and TMC207 (Figure 2), which was synergistic
285 with PA824 (ΣFIC = 0.5 - 0.625) and additive with TMC207 (ΣFIC = 0.625) based on FIC.
286
287
288 The combination of 2 with TMC207 at sub-MICs showed an additional ~1.5 log_{10}CFU
289 reduction over maximum individual drug effect (at MIC). Similarly, an additional ≥4 log_{10}CFU
290 reduction was observed with PA824 (Figure 2). In addition, the combination with
291 meropenem, rifampicin and streptomycin showed weaker synergy with the compound **2**
292 (Supplemental Figure 2). Similar results were also observed with other compounds from 1,4-

293 azaindole series published earlier.[11] Interestingly, BTZ043, which also targets DprE1
294 enzyme, exhibits synergy with TMC207.[12,17] The absence of any antagonism with a variety of
295 tested anti-TB drugs supports the potential of 1,4-azaindoles for combination therapy.
296
297 **Efficacy and *in vivo* combination study in a mouse TB infection model**
298 The *in vivo* efficacy of a representative compound (**2**) was assessed in BALB/c mice in a
299 chronic TB infection model, wherein the treatment was started on day 28, post-infection.
300 After four weeks of treatment with compound **2**, the bacterial burden in the lungs was
301 reduced by ~1 $\log_{10}$CFU/lung at 300 mg/Kg and statistically significant dose dependent
302 efficacy was observed (Figure 3). The oral exposure of compound **2**, assessed from infected
303 animals showed AUCs of 243 μM.h and total plasma concentrations above the MIC for ~ 15
304 h at the dose of 300 mg/kg (Table 3). Moreover, the compound **2** (at 100 mg/kg) was also
305 tested for *in vivo* combination efficacy with PA824 (50 mg/kg) and TMC207 (25 mg/kg) in the
306 mouse chronic TB infection model. The bacterial burden in the lungs was reduced by ~0.7
307 and ~3.5 $\log_{10}$CFU/lung in case of combination with PA824 and TMC207 respectively. Thus,
308 the synergy observed for 1,4-azaindole (**2**) with TMC207 (as estimated by CFU reduction,
309 Figure 2) *in vitro* translated to *in vivo*. However, this was not true for the combination with
310 PA824. The oral exposure of compound **2** assessed from infected animals did not change
311 significantly when given in combination with PA824 and TMC207 (Table 3). Similarly, the
312 oral exposures of PA824 and TMC207 remained unchanged when given in combination with
313 the compound **2** (Supplemental Figure 3 and Supplemental Table 1). Although streptomycin
314 and meropenem demonstrated synergy *in vitro*, they were not evaluated *in vivo* due to being
315 injectable and observed stability issues respectively. No adverse events were observed
316 during 4 weeks of repeated dosing during the study.
317
318 **Correlation of CL across species**
319 Pharmacokinetic profile of compound **1** as a representative of the series in mice, rats and
320 dogs was determined post IV and oral dosing. The compound **1** showed an oral
321 bioavailability of 86 and 100 % in rats and dogs respectively. Interestingly, the observed
322 systemic CL was within 1.5 fold of the predicted value in both rats and dogs, confirming the
323 hypothesis that hepatic route is indeed the primary route of elimination (Table 2). The
324 predicted vs observed *in vivo* CL values were within 1 fold for compound **2** in rats (Table 2).
325 Hence, 1,4-azaindoles showed good *in vitro* to *in vivo* correlation. Further, human CL was
326 predicted using IVIVC as described in materials and methods. Both the compounds (**1** & **2**)
327 were predicted to show low human CL (CLh: < 30% liver blood flow).
328 Using the observed CL in rat and dog, human CL for compound **1** was also predicted by
329 simple, two species (rat & dog) allometry (Supplemental Table 2). Predicted mean estimates

330 of human CL obtained by allometry (3.3 ml/min/kg) and IVIVC (2.9 ml/min/kg) were very
331 similar. Steady-state daily AUC required for ≥1.0 log_{10} CFU reduction in a chronic rat TB
332 model and predicted human CL, predicted ≤1 gm per day as an efficacious human dose,
333 assuming complete bioavailability for compound **2** (Table 4). This is a point estimate of the
334 predicted human dose without considering potential PK variability.
335
336 **Efficacy study in a rat TB infection model**
337 As described before, a significant challenge associated with the 1,4-azaindole series was
338 rapid metabolism in the presence of mouse liver microsomes. This made it difficult to explore
339 efficacy in mouse model of tuberculosis for compounds from 1,4-azaindole series. However,
340 all compounds in the series had low clearance and significant oral exposures in rats. This
341 allowed us to assess representative compounds for *in vivo* efficacy in a rat "chronic" TB
342 infection model as an alternate model to well established mouse model. After four weeks of
343 treatment with compounds **1** & **2**, the bacterial burden in the lungs was reduced by 0.5 to ≥ 1
344 log_{10}CFU/ left lobe of the lung and statistically significant dose dependent efficacy was
345 observed (Figure 4). The oral exposure of compounds **1** & **2**, assessed from infected
346 animals showed AUCs ranging from 166 to 240 μM•h and free plasma concentrations were
347 maintained above the MIC for 10−24 h (Table 5). No adverse events in the form of body
348 weight loss, organ weight loss, or gross pathology were observed following 4 weeks of
349 repeated dosing in the efficacy studies.
350
351 In summary, the 1,4-azaindole (**2**) was identified as a potential clinical candidate for TB
352 treatment. It also showed synergy with TMC207 and no antagonism with other anti-TB
353 drugs.

354 **References**

355 1. **Warner, D. F., and V. Mizrahi.** 2013. Complex genetics of drug resistance in
356 *Mycobacterium tuberculosis.* Nat. Genet. **45:**1107–1108.
357 2. **World Health Organization.** 2013. Global Tuberculosis Report.
358 3. **Raviglione, M., Marais, B., Floyd, K., Lönnroth, K., Getahun, H., Migliori, G.**
359 **B., Harries, A. D., Nunn, P., Lienhardt, C., Graham, S., Chakaya, J., Weyer,**
360 **K., Cole, S., Kaufmann, S. H., and A. Zumla.** 2012. Scaling up interventions to
361 achieve global tuberculosis control: progress and new developments. Lancet.
362 **379:**1902–1913.
363 4. **Lienhardta, C., Vernonb, A., and M. C. Raviglionec.** 2010. New drugs and new
364 regimens for the treatment of tuberculosis: review of the drug development pipeline
365 and implications for national programmes. Curr. Opin. Pulm. Med. **16:**186–193.
366 5. **Hett, E. C., and E. J. Rubin.** 2008. Bacterial growth and cell division: a
367 mycobacterial perspective. Microbiol. Mol. Biol. Rev. **72:**126-56.
368 6. **Lu, H., and P. J. Tonge.** 2008. Inhibitors of FabI, an Enzyme Drug Target in the
369 Bacterial Fatty Acid Biosynthesis Pathway. Acc. Chem. Res. **41:**11-20.
370 7. **Jackson, M., McNeil, M. R., and P. J. Brennan.** 2013. Progress in targeting cell
371 envelope biogenesis in *Mycobacterium tuberculosis*. Future Microbiol. **8:**855–875.
372 8. **Mikušová, K., Huang, H., Yagi, T., Holsters, M., Vereecke, D., D'Haeze,**
373 **W., Scherman, M. S., Brennan, P. J., McNeil, M. R., and D. C. Crick.** 2005.
374 Decaprenylphosphoryl arabinofuranose, the donor of the D-arabinofuranosyl
375 residues of mycobacterial arabinan, is formed via a two step epimerization of
376 decaprenylphosphoryl ribose. J. Bacteriol. **187:**8020–8025.
377 9. **Makarov, V., Manina, G., Mikusova, K., Möllmann, U., Ryabova, O., Saint-**
378 **Joanis, B., Dhar, N., Pasca, M. R., Buroni, S., Lucarelli, A. P., Milano, A., De**
379 **Rossi, E., Belanova, M., Bobovska, A., Dianiskova, P., Kordulakova, J., Sala,**
380 **C., Fullam, E., Schneider, P., McKinney, J. D., Brodin, P., Christophe,**
381 **T., Waddell, S., Butcher, P., Albrethsen, J., Rosenkrands, I., Brosch, R., Nandi,**
382 **V., Bharath, S., Gaonkar, S., Shandil, R. K., Balasubramanian, V., Balganesh,**
383 **T., Tyagi, S., Grosset, J., Riccardi, G., and S. T. Cole** 2009. Benzothiazinones kill
384 *Mycobacterium tuberculosis* by blocking arabinan synthesis. Science. **324:**801–804.
385 10. **Wang, F., Sambandan, D., Halder, R., Wang, J., Batt, S. M., Weinrick,**
386 **B., Ahmad, I., Yang, P., Zhang, Y., Kim, J., Hassani, M., Huszar, S., Trefzer,**
387 **C., Ma, Z., Kaneko, T., Mdluli, K. E., Franzblau, S., Chatterjee, A. K., Johnsson,**
388 **K., Mikusova, K., Besra, G. S, Fütterer, K., Robbins, S. H., Barnes, S.**
389 **W., Walker, J. R., Jacobs, W. R. Jr, and P. G. Schultz.** 2013. Identification of a

390 small molecule with activity against drug-resistant and persistent tuberculosis. Proc.
391 Natl. Acad. Sci. **110:**E2510–E2517.
392 11. **Shirude, P. S., Shandil, R., Sadler, C., Naik, M., Hosagrahara, V., Hameed,**
393 **S., Shinde, V., Bathula, C., Humnabadkar, V., Kumar, N., Reddy, J., Panduga,**
394 **V., Sharma, S., Ambady, A., Hegde, N., Whiteaker, J., McLaughlin, R.**
395 **E., Gardner, H., Madhavapeddi, P., Ramachandran, V., Kaur, P., Narayan,**
396 **A., Guptha, S., Awasthy, D., Narayan, C., Mahadevaswamy, J., Vishwas, K.**
397 **G., Ahuja, V., Srivastava, A., Prabhakar, K. R., Bharath, S., Kale, R., Ramaiah,**
398 **M., Choudhury, N. R., Sambandamurthy, V. K., Solapure, S., Iyer, P.**
399 **S., Narayanan, S., and M. Chatterji** 2013. Azaindoles: Noncovalent DprE1 inhibitors
400 from scaffold morphing efforts, kill *Mycobacterium tuberculosis* and are efficacious *in*
401 *vivo*. J. Med. Chem. **56:**9701-9708.
402 12. **Makarov, V., Lechartier, B., Zhang, M., Neres, J., van der Sar, A. M., Raadsen, S.**
403 **A., Hartkoorn, R. C., Ryabova, O. B., Vocat, A., Decosterd, L. A., Widmer,**
404 **N., Buclin, T., Bitter, W., Andries, K., Pojer, F., Dyson, P. J., and S. T. Cole** .2014.
405 Towards a new combination therapy for tuberculosis with next generation
406 benzothiazinones. EMBO Mol. Med. published online.
407 13. http://www.tballiance.org/downloads/Pipeline/TBA%20Pipeline%20Q1%202014(2)%
408 20(DA).pdf
409 14. **Solapure, S., Dinesh, N., Shandil, R., Ramachandran, V., Sharma,**
410 **S., Bhattacharjee, D., Ganguly, S., Reddy, J., Ahuja, V., Panduga, V., Parab,**
411 **M., Vishwas, K. G., Kumar, N., Balganesh, M., and V. Balasubramanian** 2013. *In*
412 *vitro* and *in vivo* efficacy of β-lactams against replicating and slowly growing/
413 nonreplicating *Mycobacterium tuberculosis*. Antimicrob. Agents Chemother.
414 **57:**2506–2510.
415 15. **Gaonkar, S., Bharath, S., Kumar, N., Balasubramanian, V., and R. K. Shandil**
416 .2010. Aerosol infection model of tuberculosis in Wistar rats. International journal of
417 microbiology. 426035.
418 16. **Sohlenius-Sternbeck, A. K., Jones, C., Ferguson, D., Middleton, B. J., Projean,**
419 **D., Floby, E., Bylund, J., and L Afzelius** .2012. Practical use of the regression
420 offset approach for the prediction of in vivo intrinsic clearance from hepatocytes.
421 Xenobiotica. **42**:841-853.
422 17. **Lechartier, B., Hartkoorn, R. C., and S. T. Cole.** 2012. In vitro combination studies
423 of benzothiazinone lead compound BTZ043 against Mycobacterium tuberculosis.
424 Antimicrob. Agents Chemother. **56**:5790-5793.
425
426

427 **Tables**

428 TABLE 1. The properties of shortlisted compounds from 1,4 azaindole series.

429 [a]CYP1A2, CYP2C9, CYP2C19, CYP2D6, CYP3A4, [b]panel of ~65 high and medium severity

Compound		**1**	**2**
DprE1 IC_{50} (μM)		0.010	0.032
Mtb MIC (μM)		0.78-3.12	0.5-1.56
Mtb MBC (μM)		1.56	1.56-3.12
Drug sensitive clinical isolates MIC (μM)		0.4-6.25	0.4-3.12
INH^R, RIF^R clinical isolates (μM)		0.78-3.12	0.78-1.56
DprE1 over-expression strain MIC (μM)		50-200	200
DprE1 C387S/G ($BTZ043^R$) MIC (μM)		0.78-1.56	0.78-1.56
Potency in intracellular THP1 model (log_{10}CFU reduction)		~1.5	~1.5
Cytotoxicity (μM) THP-1		>100	>100
logD		1.8	1.8
Solubility (μM)		170	464
Mouse	Microsome CL_{int} (μl/min/mg)	28	38
	CL_{pred} (ml/min/kg) (% LBF)	16 (11)	28 (18)
Human	Microsome CL_{int} (μl/min/mg)	<4	10
	CL_{pred} (ml/min/kg) (% LBF)	4 (19)	6 (30)
Rat	Hepatocyte CL_{int} (μl/min/10^6 cells)	4	5
	CL_{pred} (ml/min/kg) (% LBF)	10 (14)	12 (16)
Dog	Hepatocyte CL_{int} (μl/min/10^6 cells)	<1	<1
	CL_{pred} (ml/min/kg) (% LBF)	9 (16)	8 (15)
Human	Hepatocyte CL_{int} (μl/min/10^6 cells)	<1	<1
	CL_{pred} (ml/min/kg) (% LBF)	2 (9)	2 (11)
Human Fu_{plasma}		0.22	0.30
Caco-2 P_{app} A to B ($1E^{-6}$.cm/s)		11	5
CYP[a] inhibition (time dependent inhibition) IC_{50} (μM)		>50	>50
hERG IC_{50} (μM)		>33	>33
PDE6 IC_{50} (μM)		4	>100
Secondary pharmacology hits IC_{50} (μM)		No significant hits[b]	
Rat PK	CL (ml/min/kg) (% LBF)	27 (38)	24 (33)
	F (%)	100	87

430 targets (binding and functional data) - IC_{50} >100 µM or >30 µM
431
432 TABLE 2. Pharmacokinetic parameters of compound **1** & **2** in rats and dogs

Compound	Animal model	Hepatocyte CL_{int} (µl/min/10^6 cells)	Measured plasma CL *in vivo* (ml/min/kg)	Predicted Blood CLh (ml/min/kg)	Fold under prediction of CL
1	Rat	5.8	27	20.6	1.31
	Dog	1	6	8	0.75
2	Rat	4.8	23.7	23.3	1.02

433
434
435
436 TABLE 3. Pharmacokinetic parameters (Mean ± SD, n=3) of **2** following multiple oral dose
437 administration in Mtb infected male BALB/c mice.

PK Parameter	**2**			**2** + PA824	**2** + TMC207
Dose (mg/kg)	30	100	300	100 + 50	100 + 25
C_{max} (µM)	25.8 ± 4.1	33.6 ± 5.8	64.9 ± 8.4	26.3 ± 3.6	33.7 ± 3
AUC_{last} (µM.h)	13.4 ± 2.1	65.3 ± 10.7	243 ± 59.1	53.1 ± 7.4	46.3 ± 1.7
T_{max} (h)	0.25 ± 0	0.5 ± 0	0.3 ± 0.1	0.3 ± 0	0.3 ± 0
$T_{1/2}$ (h)	1.2 ± 0.1	2.1 ± 0.2	2 ± 0.4	2.7 ± 0.2	2.8 ± 0.4

438
439
440 TABLE 4 . Predicted mean estimates of human CL and dose assuming oral F = 1.0.

Compound	MW	Efficacious dose for ≥1 log CFU reduction in rat model (mg/kg)	Efficacious AUC_{24} in infected rats (µM.h)	Predicted Human CL (ml/min/kg)	Predicted Human dose (mg/70 kg)
2	368.4	100	166	3.6	925

441
442
443 TABLE 5. Pharmacokinetic parameters (Mean ± SD, n=3) of **1** & **2** following multiple oral
444 dose (100 mg/kg) administration in Mtb infected male Wistar rats.

PK parameter	Compounds	
	1	**2**
Dose (mg/kg)	100	100
C_{max} (µM)	46.1 ± 7.7	31.5 ± 3.0
AUC_{last} (µM.h)	986.4 ± 274.3	166.1 ± 43.9

T_{max} (h)	5.3 ± 1.2	2.0 ± 0.0
$T_{1/2}$ (h)	3.8 ± 0.6	4.6 ± 0.0

445
446
447
448
449 **Figure Legends**
450
451 FIG 1: Shortlisted compounds from 1,4 azaindole series.
452
453 FIG 2: *In vitro* combination study of compound **2** with TMC207 and PA824. For PA824 CFU
454 recovered were <200 per ml (LOQ). Fractional MICs, F_A and F_B are given in parenthesis for
455 each drug (*X = fold MIC).
456
457 FIG 3: **A**. Summary of efficacy of **2** alone and in combination with PA824 & TMC207 in a
458 chronic TB infection model in BALB/c mice following 6 days a week oral dosing for four
459 weeks. The net log_{10}CFU/lung reduction was obtained by subtracting lung bacterial counts
460 from the vehicle treated control. Compound **2** exhibited statistically significant effect at 300
461 mg/kg vs untreated controls (*$p<0.05$). The bacterial counts at the start of treatment (early
462 control) and at the end of treatment (late control) were 6.0 ± 0.08 log_{10}CFU/lung and 6.24 ±
463 0.12 log_{10}CFU/lung respectively. **B**. Time vs. concentration profiles of **2** and in combination
464 with PA824 and TMC207 following multiple oral administrations at 30, 100 & 300 mg/kg in
465 chronically Mtb infected mice.
466
467 FIG 4: **A**. Summary of efficacy of **1** & **2** in chronic TB infection model in Wistar Rats following
468 6 days a week oral dosing for four weeks. The net log_{10}CFU reduction/left lobe of the lung
469 was obtained by subtracting bacterial counts from the vehicle treated control. Both
470 compounds exhibited statistically significant effect vs untreated controls (*$p<0.05$). The
471 bacterial counts at the start of treatment (early control) and at the end of treatment (late
472 control) were 6.02 ± 0.11 log_{10}CFU/lung and 6.41± 0.20 log_{10}CFU/lung respectively. **B**. Time
473 vs. concentration profiles of **1** & **2** following multiple oral administrations at 100 mg/kg in
474 chronically Mtb infected rats.

Fig. 1

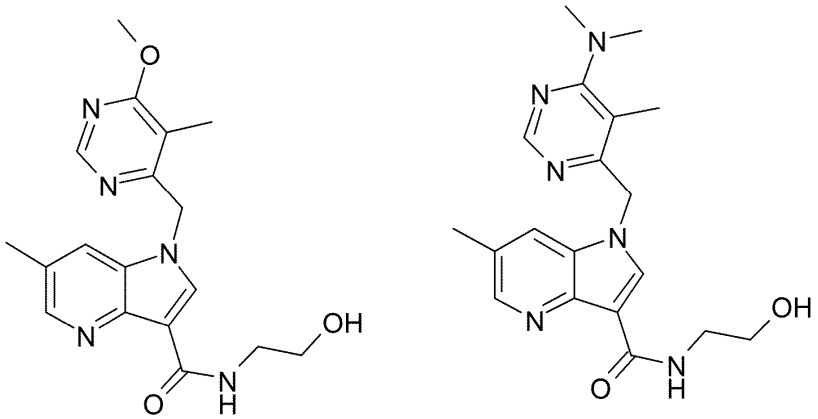

1 **2**

Fig. 2

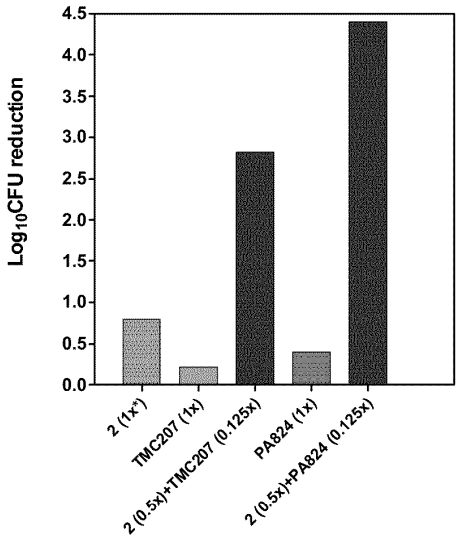

Fig. 3A

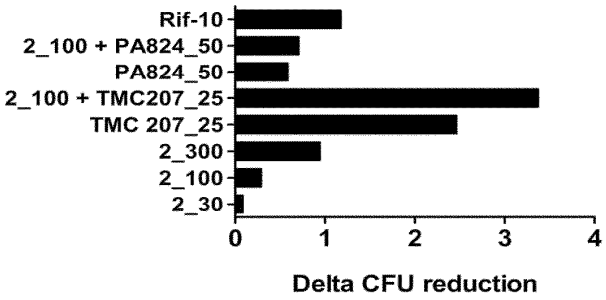

Fig. 3B

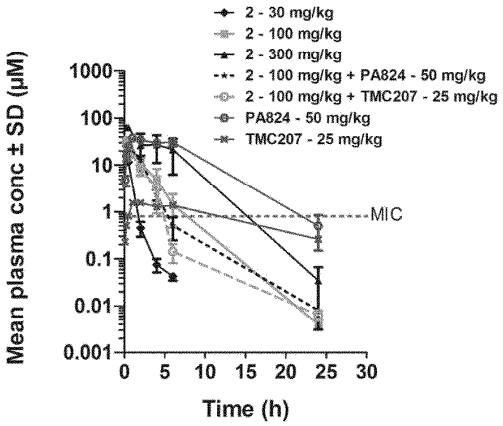

Fig. 4A

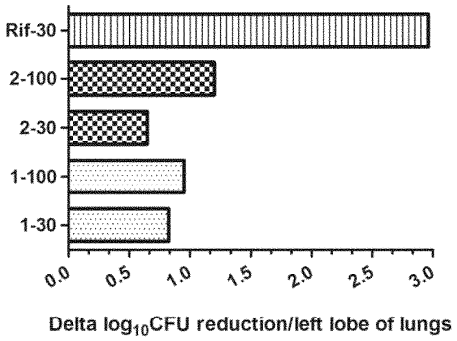

Fig. 4B